THE YOUNG UNIVERSE
ASP Conference Series, Vol. 146, 1998
S. D'Odorico, A. Fontana, E. Giallongo, eds.

Spatial distribution of the Lyα forest

Patrick Petitjean

Institut d'Astrophysique de Paris - CNRS, 98bis Bd Arago, F-75014 Paris, France

DAEC, Observatoire de Paris, 5 Place Jules Janssen, 92195 Meudon, France

Jean Surdej[1] and Marc Remy

Institut d'Astrophysique, Université de Liège, Avenue de Cointe 5, B-4000 Liège, Belgium

Alain Smette

NASA-Goddard Space Flight Center, Code 681, Greenbelt, MD 20771, USA

Jan Mücket

Astrophysikalisches Institut Potsdam, An der Sternwarte 16, D-14482 Potsdam, Germany

Peter Shaver

European Southern Observatory, Schwarzschild Strasse 2, D-80547 Garching, Germany

Abstract. The spatial distribution of the Lyα forest is studied using new HST data of the quasar pair Q 1026–0045 A and B at $z_{\rm em} = 1.438$ and 1.520 respectively. The angular separation is 36 arcsec and corresponds to transverse linear separations between lines of sight of $\sim 300 h_{50}^{-1}$ kpc ($q_{\rm o} = 0$) over the redshift range $0.833 < z < 1.438$. From the observed numbers of coincident and anti-coincident Lyα absorption lines, we conclude that, at this redshift, the Lyα structures have typical dimensions of $\sim 500 h_{50}^{-1}$ kpc, larger than the mean separation of the two lines of sight. The velocity difference, ΔV, between coincident lines is surprisingly small (4 and 8 pairs with $\Delta V < 50$ and 200 km s^{-1} respectively).
There is a metal-poor associated system at $z_{\rm abs} = 1.4420$ along the line of sight to A with complex velocity profile. We detect a strong Lyα absorption along the line of sight to B redshifted by only 300 km s^{-1} relatively to the associated system. Given the strong proximity effect from quasar A, it is tempting to interpret this as the presence of a disk of radius larger than $300 h_{50}^{-1}$ kpc surrounding quasar A.

[1]Directeur de Recherches du FNRS, Belgium

1. Introduction

One way to probe the transverse extension of the gaseous structures giving rise to the Lyα forest seen in the spectrum of quasars is to observe multiple lines of sight to quasars with small angular separations on the sky and search the spectra for absorptions coincident in redshift. This technique has been pioneered by Sargent et al. (1982) (see also Oort 1981, Weymann & Foltz 1983, Shaver & Robertson 1983). Foltz et al. (1984) derived a cloud radius larger than 50 kpc at $z \sim 2$ from the observation of Q2345+007A and B separated by 7.3 arcsec. Similar conclusions have been reached using higher resolution observations of other pairs of quasars (Smette et al. 1992, Dinshaw et al. 1994, Bechtold et al. 1994, Crotts et al. 1994, Bechtold & Yee 1994, Smette et al. 1995).
Most of the pairs are double images of lensed quasars and thus have small angular separations. Since the structures are large, these pairs are useful to probe the small scale structure of the clouds but their angular separations are too small to derive the total extension and the spatial distribution of the gas on large scales. Recently, Dinshaw et al. (1995) derived a radius of 330 kpc at $z \sim 0.7$ for spherical clouds from observation of Q0107–0232 and Q0107–0235 separated by 86 arcsec. Larger separations have been investigated by Crotts & Fang (1997) and Williger et al. (1997). Both studies conclude that the clouds should be correlated on scales larger than 500 kpc.
Here we present preliminary results of a study of the pair Q1026–005 A ($m_{\rm r} = 18.4$, $z_{\rm em} = 1.438$) and B ($m_{\rm r} = 18.5$, $z_{\rm em} = 1.520$), a real quasar pair with a separation of 26 arcsec or 300 h_{50}^{-1} kpc at $z \sim 1$. The observations were carried on the Hubble Space Telescope with the Faint Object Spectrograph using the G270H grating over the wavelength range 2250–3250 Å, for a resolution of 1.92 Å FWHM. A total of 5300 s integration time was accumulated on both quasars Q1026–0045A and B. Multi-object spectroscopy was performed on the galaxies in the field using EMMI on the ESO NTT at the La Silla observatory.

2. The Lyα forest

We detect 12 and 11 Lyα lines with rest equivalent widths $w_{\rm r} > 0.2$ Å over the redshift range 0.8335–1.3436 along the lines of sight to A and B respectively. The density of lines with $w_{\rm r} > 0.24$ Å detected in the course of the HST Key-Programme "Absorption Line Systems" over the same redshift range is $\sim$33$\pm$3 (Jannuzi et al. 1998). The number of lines we detect is thus small. This might be partly a consequence of blending effects.
Two absorption lines from different lines of sight are considered coincident when their redshifts differ by less than 200 km s^{-1}. The numbers of coincidences and anticoincidences for $w_{\rm r} > 0.2$, 0.3 and 0.6 Å are 4, 3, 1 and 9, 8, 3 respectively. Assuming that the Lyα clouds are spheres of radius R, we calculate the density probability for R (see Fig. 1) following Bechtold et al. (1994). The peak of the probability is at $R = 262$, 248 and $228 h_{50}^{-1}$ kpc for the three subsamples. There is a hint for the dimensions of the structures to be larger for smaller equivalent widths. This indicates that the clouds are of very large dimensions although these numbers should be considered as indicative since the Lyα structures are most certainly elongated and clustered.

We used simulations (Mücket et al. 1996, Riediger et al. 1997) to compute the probability to find a coincidence (within 200 km s^{-1}) along two lines of sight taken at random in the simulation box. This probability is plotted versus the separation between the lines of sight in Fig. 1 (lower panel) for various column density thresholds. The slow decrease of the probability with separation results from the gas being distributed in filamentary structures (see Fig. 2 lower panel). Observational data are overplotted (see Section 1 for references) and there is a definite indication that the observations, although sparse, are consistent with the model.

It is interesting to note that the velocity difference between coincident lines is very small. We find 8 and 4 coincidences with velocity separations smaller than 200 and 50 km s^{-1} (see Fig. 2 upper panel). This is expected if the absorptions arise in thin sheets, generally perpendicular to both lines of sight. This question should be investigated in more detail however.

Finally, we searched for galaxies in the field possibly associated with absorption lines. Our observational run was not very successful. We found however a galaxy at $z = 0.9512$, 490 and 440 kpc away from B and A respectively, possibly associated with the absorptions at $z = 0.9486$ in B and $z = 0.9486$ and 0.9536 in A (see Fig. 3).

3. The associated system in A

There is a strong associated system detected in A by its H I Lyα and Lyβ absorptions. Two components are seen at $z_{\rm abs} = 1.4401$ and 1.4420 with $w_{\rm r}({\rm Ly}\alpha) = 0.58$ and 0.40 Å (marked as components *a* and *b* in Fig. 4). The two components are *redshifted* relative to the QSO emission lines by 260 and 490 km s^{-1}. Since the true redshift of the quasar is poorly known, these values are very uncertain. We do not detect any metal lines in the system. The O VI lines have $w_{\rm r} < 0.20$ Å; the C IV lines are redshifted outside the wavelength range of the data. Interestingly enough, there is a H I Lyα absorption line at $z_{\rm abs} = 1.4439$ along the line of sight to Q 1026–0045B (marked as component *c* in Fig. 4). The velocity difference between this line and the $z_{\rm abs} = 1.4420$ component in A is about 230 km s^{-1} only.

It is unlikely that the $z_{\rm abs} \sim z_{\rm em}$ system is intrinsically associated with the central AGN. Such systems usually have high metal content and are expected to exhibit strong O VI and N V absorptions (e.g. Petitjean et al. 1994), absent from the spectra of Q1026–0045 A & B. The three absorptions are thus part of an object or group of objects which transversal dimension exceeds the $300h_{50}^{-1}$ kpc separation between the two lines of sight.

The absence of metals in the system associated with A, over the observed wavelength range, suggests an intergalactic origin. The higher velocity of the gas along the line of sight to B argues against the simple picture in which the gas would be collapsing toward A. In that case, we would expect the gas along the line of sight to B to have a projected velocity smaller than the velocity of the gas just in front of A. A model where the gas would be part of a rotating disk can be accomodated if the component at $z = 1.4420$ is at the same redshift as the quasar (see bottom panel in Fig. 4).

The relative equivalent widths of the hydrogen lines in the Lyman series at $z = 1.4842$ are indicative of H I column densities in excess of 10^{16} cm^{-2}. The presence of strong metal lines suggests that the gas is associated with the halo of a galaxy. Very deep imaging in this field to search for any enhanced density of objects would help to understand the nature of these intriguing systems.

4. Proximity effect

There are only two Lyα absorption lines along both lines of sight from $z = 1.3436$ to 1.520, the associated system in A (and its counterpart in B) and the metal system at $z = 1.4842$ in B. The number of lines with $w_r > 0.24$ Å expected in this redshift range is 7±2 (Bahcall et al. 1996). It is probable that we see the effect of the enhanced photo-ionizing field due to the proximity of the quasars.

Acknowledgments. This work is partly based on observations obtained with the NASA/ESA *Hubble Space Telescope* by the Space Telescope Institute, which is operated by AURA, Inc., under NASA contract NAS 5-26555.

References

Bahcall, J. N., et al. 1996, ApJ, 457, 19

Bechtold, J., Crotts, A. P. S., Duncan, R. C., & Fang, Y. 1994, ApJ, 437, L83

Bechtold, J., & Yee, H. K. C. 1994, AJ, 110, 1984

Crotts, A. P. S., Bechtold, J., Fang, Y., & Duncan, C. 1994, ApJ, 437, 79

Crotts, A. P. S., & Fang, Y. 1997, astro-ph 9702185

Dinshaw, N., Foltz, C. B., Impey, C. D., Weymann, R. J., & Morris, S. L. 1995, Nature, 373, 223

Dinshaw, N., Impey, C. D., Foltz, C. B., Weymann, R. J., & Chaffee, F. H. Jr. 1994, ApJ, 437, L87

Fang, Y., Duncan, R. C., Crotts, A. P. S., & Bechtold, J. 1996, ApJ, 462, 77

Foltz, C. B., Weymann, R. J., Röser, H. J., & Chaffee, F. H. Jr. 1984, ApJ, 281, L1

Jannuzi, B. T., et al. 1998, ApJS, in press

Mücket, J. P., Petitjean, P., Kates, R. E., & Riediger, R. 1996, A&A, 308, 17

Oort, J. H. 1981, A&A, 94, 359

Petitjean, P., Rauch, M., & Carswell, R. F. 1994, A&A, 291, 29

Riediger, R., Petitjean, P., & Mücket, J. P. 1997, astro-ph/9709131

Sargent, L. W. L., Young, P., & Schneider, D. P. 1982, ApJ, 256, 374

Shaver, P. A., & Robertson, J. G. 1983, ApJ, 268, L57

Smette, A., et al. 1992, A&A, 389, 39

Smette, A., et al. 1995, A&AS, 113, 199

Weymann, R. J., & Foltz, C. B. 1983, ApJ, 272, L1

Williger, G. M., Smette, A., Hazard, C., Baldwin J. A., & McMahon R. G. 1997, astro-ph/9709170

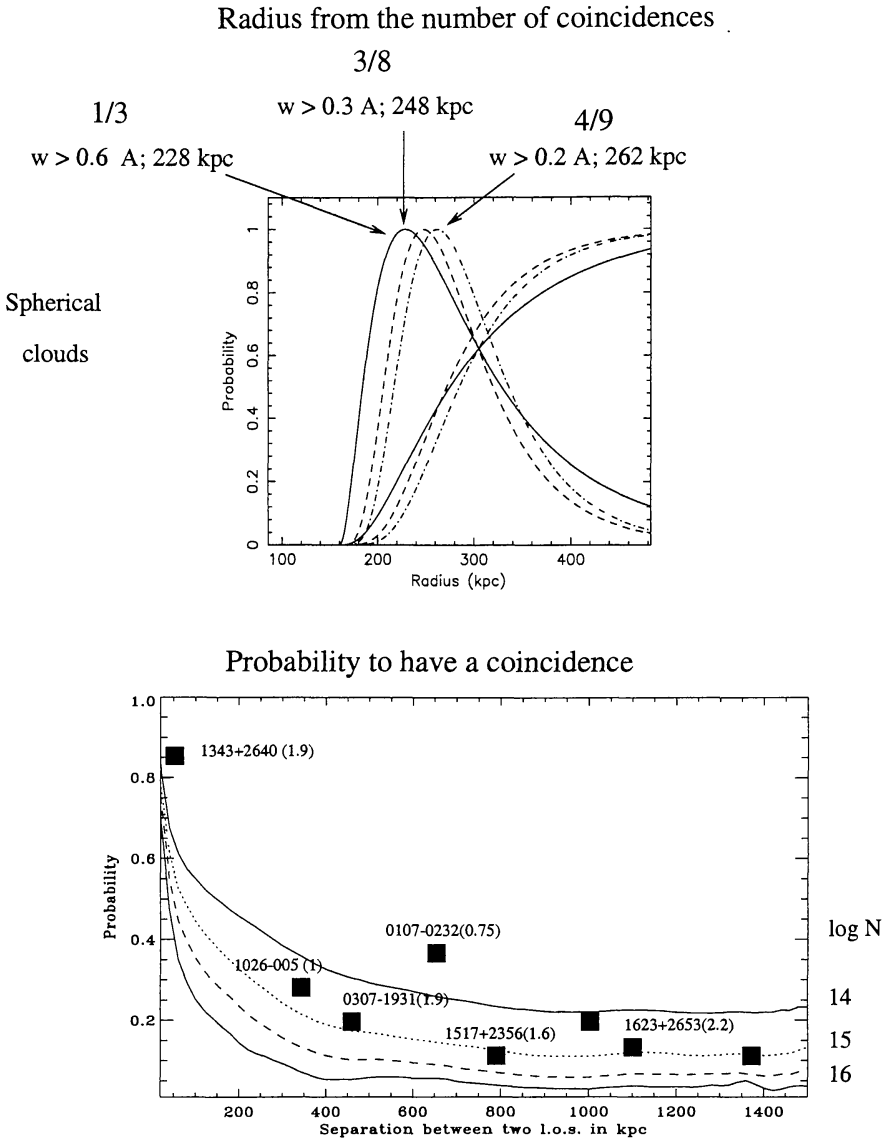

Figure 1. Top panel: Probability distributions normalized to one at their peak, and cumulative distributions versus cloud radius from the number of coincidences and anticoincidences in Q1026-0045A,B for different equivalent width limits. Lyα clouds are assumed spherical. Bottom panel: Probability to observe a coincidence in two lines of sight versus separation between the lines of sight, computed from a simulation (Mücket et al. 1996, Riediger et al. 1997). Observational data are overplotted, the number within brackets indicates the mean redshift (see Section 1 for references).

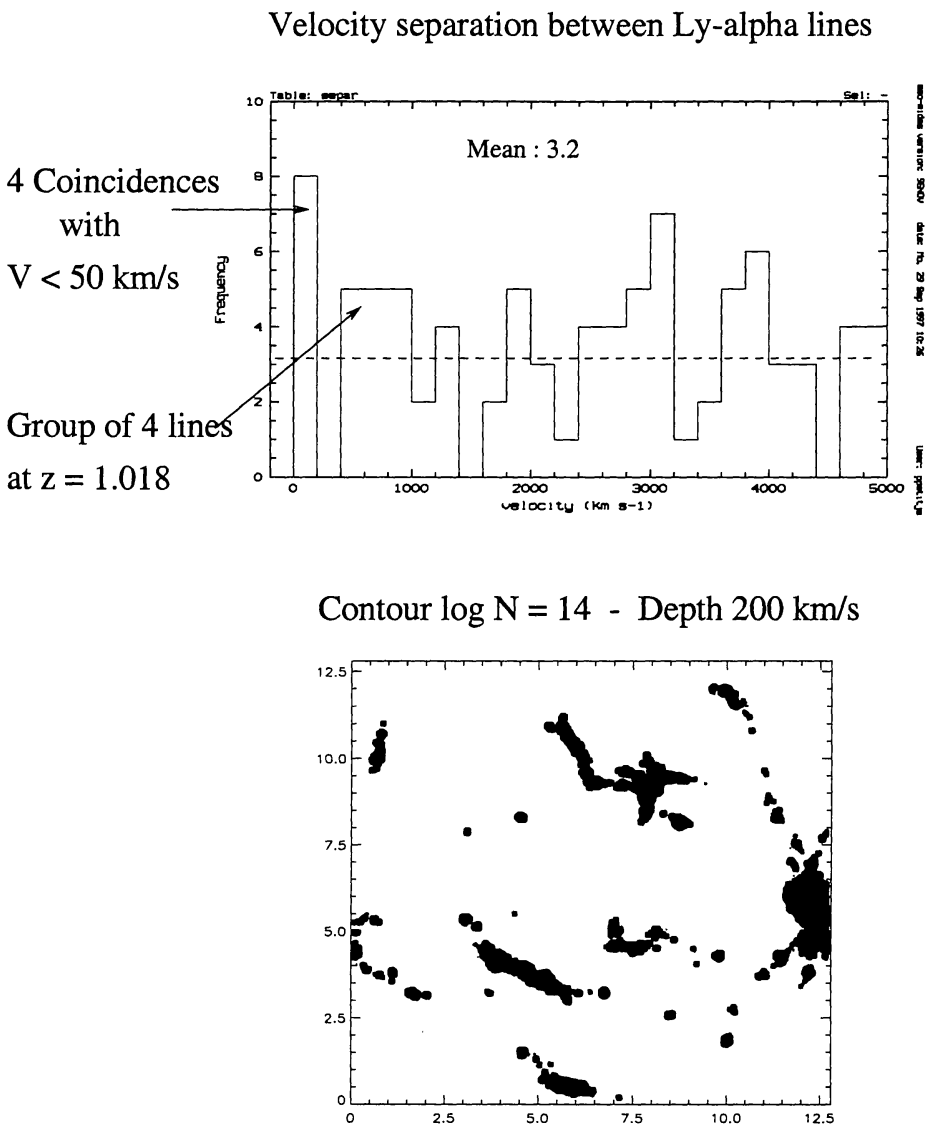

Figure 2. Top panel: Number of absorption pairs versus the velocity separation between the two lines. There are 8 and 4 pairs with velocity separations smaller than 200 and 50 km s^{-1} respectively. Bottom panel: 2D distribution of the Lyα forest with log $N > 14$ as computed from numerical simulations in a box of size 12.5 Mpc and depth 200 km s^{-1}.

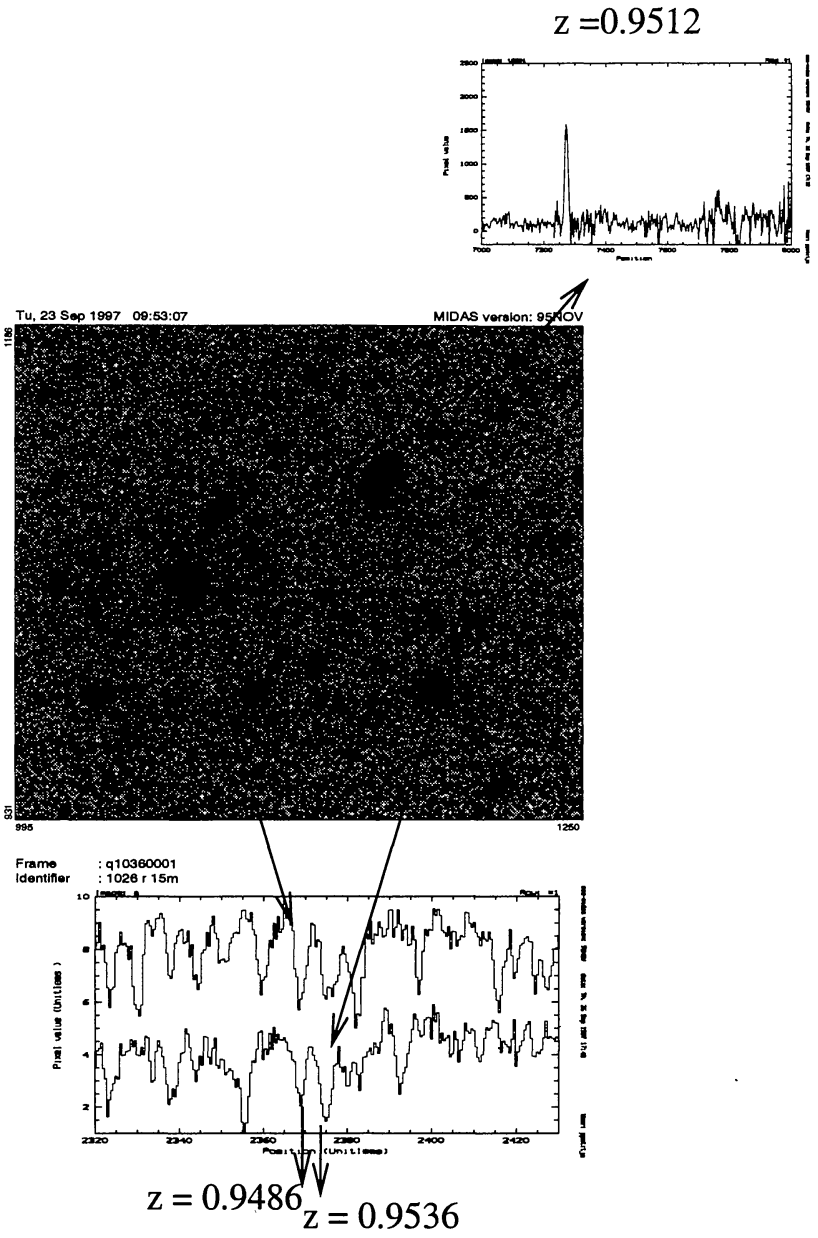

Figure 3. Detection of a galaxy at $z = 0.9512$ in the field of Q1026–0025A ($z_{\rm em} = 1.438$; situated in the bottom right corner of the image) and B ($z_{\rm em} = 1.526$; 36 arcsec or $320h_{50}^{-1}$ kpc away from A in the north east direction). North is at the top, east on the left. Lyα absorption is seen at $z = 0.9486$ and 0.9536 in A and at $z = 0.9486$ in B.

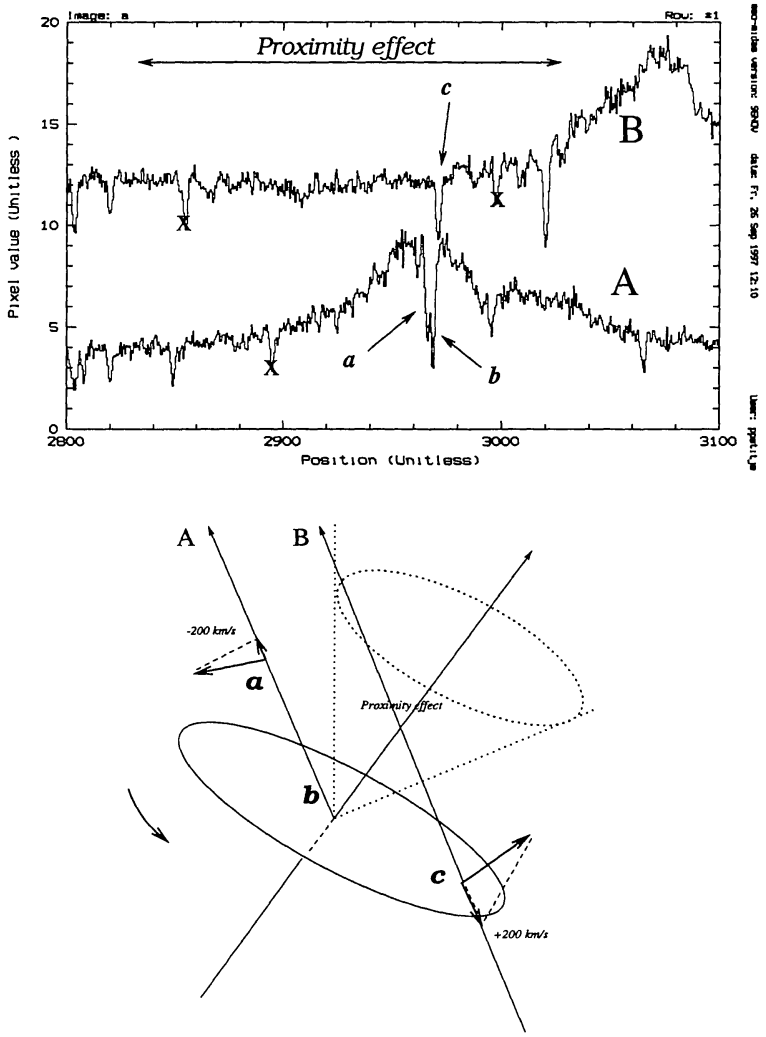

Figure 4. Top panel: Spectra of Q1026–0025A and B in the vicinity of the Lyα emission lines. There is an associated system in A with two components (labelled *a* and *b*) separated by 230 km s^{-1}. The line of sight to B passes $320h_{50}^{-1}$ kpc away from A and shows a Lyα absorption (labelled *c*) redshifted by 230 km s^{-1} relative to component *b*. Note the lack of absorption lines in the vicinity of the quasars. Lines marked by an **X** are metal lines. The absorption line at 3020 Å in B is H I Lyα associated with a strong metal line system at $z_{\rm abs} = 1.4842$. Bottom panel: Sketch of a possible configuration to explain the kinematics of the observed components seen in the associated system. Component *b* is assumed at the redshift of the quasar and components *a* and *c* are part of a large rotating disk.